

## Supporting Information

# Influenza A M2 Transmembrane Domain Tunes its Conformational Heterogeneity and Structural Plasticity in the Lipid Bilayer by Forming Loop Structures

Yue Liu,<sup>a</sup> Junjun Tan<sup>a</sup>, Jiahui Zhang<sup>a</sup>, Chuanzhao Li<sup>a</sup>, Yi Luo<sup>a</sup>, Shuji Ye,<sup>a,\*</sup>

<sup>a</sup>Hefei National Laboratory for Physical Sciences at the Microscale, and Synergetic Innovation Center of Quantum Information & Quantum Physics, University of Science and Technology of China, Hefei, Anhui 230026, China

## 1. Materials

M2TM (sequence: Ser-Ser-Asp-Pro-Leu-Val-Val-Ala-Ala-Ser-Ile-Ile-Gly-Ile-Leu-His-Leu-Ile-Leu-Trp-Ile-Leu-Asp-Arg-Leu) with a purity of >98% were purchased from Shanghai Apeptide Co., Ltd. The lipids of 1,2-dilauroyl-*sn*-glycero-3-phospho-(1'-*rac*-glycerol) (sodium salt) (DLPG), 1-palmitoyl-2-oleoyl-*sn*-glycero-3-phospho-(1'-*rac*-glycerol) (sodium salt) (POPG), 1,2-dimyristoyl-*sn*-glycero-3-[phospho-*rac*-(1-glycerol)] (sodium salt) (DMPG), 1,2-distearoyl-*sn*-glycero-3-phospho-(1'-*rac*-glycerol) (sodium salt) (DSPG), were purchased from Avanti Polar Lipids (Alabaster, AL). The hydrochloric acid (HCl) was purchased from Sinopharm Chemical Reagent Co., Ltd. The stock solution with different pH was prepared by diluting the HCl solution into ultrapure water from a Milli-Q reference system (Millipore, Bedford, MA). M2TM was dissolved in methanol and stored at -18 °C. The phospholipids were prepared in mixed solvents of chloroform and methanol (with a volume ratio of 2:1) (purchased from Sinopharm Chemical Reagent Co., Ltd.). All of the lipid solution was kept at -18 °C. Right-angle CaF<sub>2</sub> prisms were purchased from Chengdu Ya Si Optoelectronics Co., Ltd (Chengdu, China).

CaF<sub>2</sub> prisms were thoroughly cleaned using a procedure with several steps: They were first soaked in toluene for at least 24 h and then sonicated in soap detergent solution for 0.5 h. After that, they were rinsed with deionized (DI) water before soaking in methanol for 10 min. All of the

prisms were then rinsed thoroughly with an ample amount of DI water and cleaned inside Harrick plasma chamber for 10 min immediately before depositing lipid molecules on them. Substrates were tested using SFG and no signal from contamination was detected.

## 2. Sample Preparation and SFG-VS Experiments

Single lipid bilayers were prepared on CaF<sub>2</sub> substrates using Langmuir-Blodgett and Langmuir-Schaefer (LB/LS) methods with a KSV mini trough LB system.<sup>1</sup> Lipid bilayers were immersed in water inside a 2 mL reservoir throughout the entire experiment. The membrane-bound M2TM was prepared by interacting M2TM with CaF<sub>2</sub> prism-supported lipid bilayer at 24°C. A magnetic micro stirrer was used to ensure a homogeneous concentration of M2TM molecules in the subphase below the bilayer. The peptide without inserting into lipid bilayer was carefully removed by replacing the DI water or acid solution in the subphase. The SFG setup is similar to that described in our earlier publication.<sup>2</sup> All SFG experiments were carried out at the room temperature (24 °C). IR beams were protected by a home-built chamber purged with dry gas (dry gas generator, Peak Scientific) to avoid the IR energy loss due to water vapor absorptions. The high voltage applied to the detector of PMT was 1100 V for amide III signals and 700 V for amide I signals. The SFG spectra of amide I and amide III with different polarization combinations of ssp (s-polarized SFG output, s-polarized visible input, and p-polarized infrared input), ppp, and psp were collected after injecting M2TM solution into lipid bilayer and reaching equilibrium. All SFG spectra were averaged over 100 times at each point and normalized by the intensities of the input IR and visible beams.

## 3. Fitting of SFG-VS Signal

The SFG spectra were fitted using the standard procedure described by Eq. (S1).<sup>3,4</sup>

$$\chi_{eff}^{(2)}(\omega) = \chi_{NR}^{(2)} + \sum_{\nu} \frac{A_{\nu}}{\omega - \omega_{\nu} + i\Gamma_{\nu}} \quad (S1)$$

where  $A_{\nu}$ ,  $\omega_{\nu}$ , and  $\Gamma_{\nu}$  are the strength, resonant frequency, and damping coefficient of the vibrational mode ( $\nu$ ), respectively.  $A_{\nu}$  could be either positive or negative depending on the phase of the vibrational mode.  $A_{\nu}$ ,  $\omega_{\nu}$ , and  $\Gamma_{\nu}$  can be extracted by fitting the spectrum.

#### 4. Table S1- S3

**Table S1.** The structures of M2 determined by different methods

| Construct           | PDB ID | Environment    | pH/T     | loop           | Method                     |
|---------------------|--------|----------------|----------|----------------|----------------------------|
| 22-46               | 1MP6   | DMPC(P/L=1/16) | 7.0/42°C | -              | ssNMR <sup>5</sup>         |
| 22-46               | 1NYJ   | DMPC(P/L=1/8)  | 7.0/38°C | -              | ssNMR <sup>6</sup>         |
| 26-43               | 2H95   | DMPC/DMPG      | 8.8/25°C | -              | ssNMR <sup>7</sup>         |
| 22-46               | 2KAD   | DLPC(P/L=1/15) | 7.5/30°C | -              | ssNMR <sup>8</sup>         |
| 18-60,S31N          | 2KIH   | DHPC           | 7.5/30°C | 18-23,47-49,60 | ssNMR <sup>9</sup>         |
| 22-46               | 2KQT   | DMPC           | 7.5/30°C | 22-23          | ssNMR <sup>10</sup>        |
| 23-60,V27A,<br>C50S | 2KWX   | DHPC           | 7.5/30°C | 23,47-48,60    | Solution NMR <sup>11</sup> |
| 19-62,C50S          | 2L0J   | DOPC/DOPE      | 7.5/30°C | 19-22, 62      | ssNMR <sup>12</sup>        |
| 19-49,S31N          | 2LY0   | DOPC           | 6.8/40°C | 19-23, 48-49   | Solution NMR <sup>13</sup> |
| 19-49,S31N          | 2MUV   | DOPC           | 6.8/40°C | 19-23,49       | Solution NMR <sup>14</sup> |
| 19-49               | 2MUW   | DOPC           | 7.5/40°C | 19-23,49       | Solution NMR <sup>14</sup> |
| 18-60,S31N          | 2N70   | DPPC(P/L=1/1)  | 7.8/R°C  | 18-23,48-60    | NMR <sup>15</sup>          |
| 18-60,C50S          | 2RLF   | DHPC           | 7.5/30°C | 18-23,49-50,60 | Solution NMR <sup>16</sup> |
| 22-47,I33M          | 3BKD   | OP/PEG         | 7.3/100K | 22-23,47       | X-ray,2.05Å <sup>17</sup>  |
| 22-46,G34A          | 3C9J   | OG/PEG         | 5.3/100K | 22-23,41-46    | X-ray,3.5Å <sup>17</sup>   |
| 25-47,G34A          | 3LBW   | OG/PEG         | 6.5/100K | 47             | X-ray,1.65Å <sup>18</sup>  |
| 21-47               | 4QK7   | OG/PEG         | 8.0/100K | 21-23,47       | X-ray,1.10Å <sup>19</sup>  |
| 21-47               | 4QKC   | OG/PEG         | 5.5/100K | 21-23,47       | X-ray,1.10Å <sup>19</sup>  |
| 21-47               | 4QKL   | OG/PEG         | 8.0/0°C  | 21-23,47       | X-ray,1.71Å <sup>19</sup>  |
| 21-47               | 4QKM   | OG/PEG         | 5.5/0°C  | 21-23,47       | X-ray,1.44Å <sup>19</sup>  |
| 21-47,S31N          | 5C02   | OG/PEG         | 8.0/100K | 21-23,47       | X-ray,1.59Å <sup>20</sup>  |

**Table S2.** The orientation of M2 in membrane determined by different methods

| Construct           | PDB ID | Environment  | Thickness | pH/T       | Tilt angle | Method                        |
|---------------------|--------|--------------|-----------|------------|------------|-------------------------------|
| 22-46               |        | DLPC bilayer | 19.5Å     | 7.5        | 35±3       | NMR <sup>21</sup>             |
| 22-46               |        | POPC bilayer | 26.5      | 7.5        | 26±3       | NMR <sup>21</sup>             |
| 22-46               |        | DMPC bilayer | 23.0      | ~7/25°C    | 37±3       | ssNMR <sup>22</sup>           |
| 22-46               |        | DOPC bilayer | 27.0      | ~7/25°C    | 33±3       | ssNMR <sup>22</sup>           |
| 22-62,C50S          | 2L0J   | DOPC/DOPE    | 27.0      | 7.5/30°C   | 32N,22C    | ssNMR <sup>12</sup>           |
| 22-46               | 1NYJ   | DMPC bilayer | 23.0      | 7.0/38°C   | 38         | ssNMR <sup>6</sup>            |
| 22-46               | 2H95   | DMPC bilayer | 23.0      | 8.8        | 30N,21C    | ssNMR <sup>7</sup>            |
| 22-46               | 2KQT   | DMPC bilayer | 23.0      | 7.5        | 32N,18C    | ssNMR <sup>10</sup>           |
| 26-62               |        | DMPC/DMPG    | 23.0      | pH8.0/43°C | 25N,80C    | ssNMR <sup>23</sup>           |
| 22-46,I33M          | 3BKD   | OG/PEG       |           | 7.3/100K   | 33         | X-ray,2.05Å <sup>17</sup>     |
| 22-46,G34A          | 3C9J   | OG/PEG       |           | 5.3/100K   | 38         | X-ray,3.5Å <sup>17</sup>      |
| 25-46,G34A          | 3LBW   | OG/PEG       |           | 6.5/100K   | 31N,19C    | X-ray,1.65Å <sup>18</sup>     |
| 18-60,C50S          | 2RLF   | DHPC micell  | 30        | 7.5        | 16         | Solution<br>NMR <sup>16</sup> |
| 18-60,V27A,<br>C50S | 2KWX   | DHPC micell  | 30        | 7.5        | 15         | Solution<br>NMR <sup>11</sup> |
| 22-46               | 2KAD   | DLPC         | 19.5Å     | 7.5        | 38         | ssNMR <sup>8</sup>            |
| 18-60,S31N          | 2KIH   | DHPC         | 30        | 7.5/30°C   |            | ssNMR <sup>9</sup>            |
| 22-46               |        | OG/DMPC      |           | 7.0        | 31.6±6.2   | ATR-FTIR <sup>24</sup>        |
| 22-46               | 1MP6   | DMPC         | 23.0      | 7.0        | 38         | ssNMR <sup>5</sup>            |

**Table S3.** The fitting parameters of amide III SFG spectra of M2TM in Fig. 1B\*

| bilayer | polarization | $A_v$       | $\omega_v$ (cm <sup>-1</sup> ) | $\Gamma_v$ (cm <sup>-1</sup> ) | $\chi_{Peak 1}^{(2)}/\chi_{Peak 2}^{(2)}$ |
|---------|--------------|-------------|--------------------------------|--------------------------------|---|
| DLPG    | Peak 1       | 7.96(±0.5)  | 1261.2                         | 18.0                           | 0.45±0.03                                 |
|         | Peak 2       | 14.15(±0.6) | 1288.8                         | 14.4                           |   |
| DMPG    | Peak 1       | 1.72(±0.2)  | 1258.0                         | 10.0                           | 0.25±0.03                                 |
|         | Peak 2       | 10.47(±0.2) | 1292.1                         | 15.0                           |   |
| POPG    | Peak 1       | 2.61(±0.4)  | 1258.0                         | 18.0                           | 0.20±0.03                                 |
|         | Peak 2       | 11.06(±0.3) | 1293.5                         | 15.0                           |   |
| DSPG    | Peak 1       | 9.6(±1.0)   | 1234.4                         | 37.9                           | 0.59±0.06                                 |
|         | Peak 2       | 9.0(±0.6)   | 1288.0                         | 21.1                           |   |

\*The error margin is determined according to the fitting deviation of the fitting peak strength.

## 5. The helix tilt and rotation angle of M2TM in lipid bilayer

The molecular orientation information of fully  $\alpha$ -helical structure can be obtained by relating SFG susceptibility tensor elements  $\chi_{ijk}(i, j, k = x, y, z)$  to the SFG molecular hyperpolarizability tensor elements  $\beta_{lmn}(l, m, n = a, b, c)$  via the Euler z-x-z transformation(Eq.(S2)).<sup>25-28</sup> In Eq.(S2),  $N_s$  is the number of molecules at the interface,  $q$  is the vibrational mode ( $q$ ). The Euler transformation used here has a matrix in the form shown in Eq. (S3). The Euler angles  $\theta$  (tilt angle),  $\psi$  (twist angle),  $\phi$  (in-plane rotation angle) are defined in Fig.S1A.

$$\chi_{ijk,q}^{(2)} = \sum_{l,m,n} N_s \langle R_{il} R_{jm} R_{kn} \rangle \beta_{lmn,q}$$

(S2)

$$\langle R_{il} R_{jm} R_{kn} \rangle = \begin{pmatrix} -\cos(\theta) \sin(\psi) \sin(\phi) + \cos(\psi) \cos(\phi) & -\cos(\theta) \cos(\psi) \sin(\phi) - \sin(\psi) \cos(\phi) & \sin(\theta) \sin(\phi) \\ \cos(\theta) \sin(\psi) \cos(\phi) + \cos(\psi) \sin(\phi) & \cos(\theta) \cos(\psi) \cos(\phi) - \sin(\psi) \sin(\phi) & -\sin(\theta) \cos(\phi) \\ \sin(\theta) \sin(\psi) & \sin(\theta) \cos(\psi) & \cos(\theta) \end{pmatrix} \quad (S3)$$

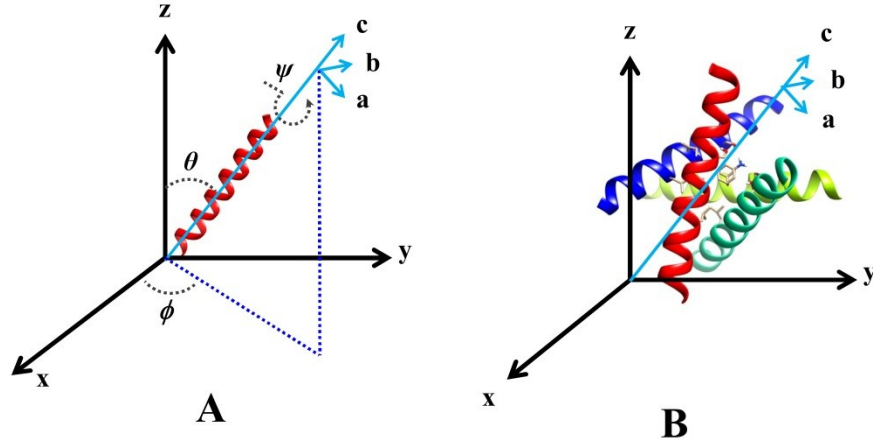


**Fig. S1** A) Euler angles ( $\theta$ ,  $\psi$ ,  $\phi$ ) relating the molecular (a, b, c) and macroscopic (x, y, z) coordinate systems. B) M2TM tetramer in the macroscopic (x, y, z) coordinate system.

The M2TM forms  $\alpha$ -helical tetramer (Fig.S1B) which has a  $C_4$  symmetry.<sup>12,16,17</sup> When the Euler angles of one of the helix is ( $\theta$ ,  $\psi$ ,  $\phi$ ), the angles of other helixes will be ( $\theta$ ,  $\psi$ ,  $\phi+90^\circ$ ), ( $\theta$ ,  $\psi$ ,  $\phi+180^\circ$ ) and ( $\theta$ ,  $\psi$ ,  $\phi+270^\circ$ ), respectively. To simplify the calculation, we can take  $\phi$  as zero. The values of all the 27 molecular hyperpolarizability elements of tetramer ( $\beta_{tetramer,abc}$ ) are thus determined by summing up the four corresponding helical hyperpolarizability elements ( $\beta_{abc}$ ) using the following equation:

$$\beta_{tetramer,abc} = \sum_{i=1}^4 \beta_{i^{th}abc} \quad (S4)$$

The total hyperpolarizability elements of tetramer for the A mode and E mode are given by,  
For the A mode:

$$\begin{aligned} \beta_{tetramer,aac} &= \beta_{tetramer,bbc} = 4\beta_{aac} = 4\beta_{bbc} \\ \beta_{tetramer,aca} &= \beta_{tetramer,bcb} = \beta_{tetramer,caa} = \beta_{tetramer,cbb} \\ &= 4\beta_{aca} = 4\beta_{bcb} = 4\beta_{caa} = 4\beta_{cbb} \\ \beta_{tetramer,ccc} &= 4\beta_{ccc} \end{aligned} \quad (S5)$$

For the E mode:

$$\beta_{tetramer,aac} = \beta_{tetramer,bbc} = 4\beta_{aac} = 4\beta_{bbc}$$

$$\begin{aligned}
\beta_{tetramer,aca} &= \beta_{tetramer,bcb} = \beta_{tetramer,caa} = \beta_{tetramer,cbb} \\
&= 4\beta_{aca} = 4\beta_{bcb} = 4\beta_{caa} = 4\beta_{cbb} \\
\beta_{tetramer,ccc} &= 4\beta_{ccc}
\end{aligned} \tag{S6}$$

Taking the tetramer as a whole, the following equations can be derived.<sup>25-28</sup>

For the A mode:

$$\chi_{A,xxz}^{(2)} = \chi_{A,yyz}^{(2)} = 2N_s^t [(1+r) \langle \cos \theta \rangle - (1-r) \langle \cos^3 \theta \rangle] \beta_{ccc} \tag{S7}$$

$$\chi_{A,xzx}^{(2)} = \chi_{A,yzy}^{(2)} = \chi_{A,zxx}^{(2)} = \chi_{A,zyy}^{(2)} = 2N_s^t [(1-r) (\langle \cos \theta \rangle - \langle \cos^3 \theta \rangle)] \beta_{ccc} \tag{S8}$$

$$\chi_{A,zzz}^{(2)} = 4N_s^t [r \langle \cos \theta \rangle + (1-r) \langle \cos^3 \theta \rangle] \beta_{ccc} \tag{S9}$$

For the E<sub>1</sub> mode:

$$\chi_{E_1,xxz}^{(2)} = \chi_{E_1,yyz}^{(2)} = -4N_s^t [\langle \cos \theta \rangle - \langle \cos^3 \theta \rangle] \langle \sin^2 \psi \rangle \beta_{aca} \tag{S10}$$

$$\chi_{E_1,xzx}^{(2)} = \chi_{E_1,yzy}^{(2)} = \chi_{E_1,zxx}^{(2)} = \chi_{E_1,zyy}^{(2)} = 4N_s^t [\langle \cos \theta \rangle \langle \sin 2\psi \rangle / 2 + \langle \cos^3 \theta \rangle \langle \sin^2 \psi \rangle] \beta_{aca} \tag{S11}$$

$$\chi_{E_1,zzz}^{(2)} = 8N_s^t [\langle \cos \theta \rangle - \langle \cos^3 \theta \rangle] \langle \sin^2 \psi \rangle \beta_{aca} \tag{S12}$$

where  $r = \beta_{aac}/\beta_{ccc}$ , and  $\beta_{aac}$ ,  $\beta_{aca}$  and  $\beta_{ccc}$  are the molecular hyperpolarizability elements of helical monomer.  $N_s^t$  is the tetramer number. The hyperpolarizability elements of an  $\alpha$ -helix can be obtained from the product of the components of the Raman polarizability and IR transition dipole moment.

Due to the limited resolution of many SFG spectrometers ( $\sim 5 \text{ cm}^{-1}$  or more), the A mode and E<sub>1</sub> mode cannot be readily resolved in the frequency domain, and therefore, the total susceptibility is often assumed to be the sum of the susceptibilities from these two modes:<sup>26-28</sup>

$$\chi_{yyz}^{(2)} = \chi_{A,yyz}^{(2)} + \chi_{E_1,yyz}^{(2)} \tag{S13}$$

$$\chi_{zzz}^{(2)} = \chi_{A,zzz}^{(2)} + \chi_{E_1,zzz}^{(2)} \tag{S14}$$

The Chen lab has developed a methodology to determine the orientation of  $\alpha$ -helical monomer structure using SFG amide I spectra collected with different polarization combinations.<sup>26-28</sup> The components of  $\chi_{eff}^{(2)}$  of ssp, and ppp polarization combinations are given in Eqs. (S15)-(S16) in the lab coordinate system which is defined as the z-axis being along the surface normal and the x-axis being in the incident plane.

$$\chi_{eff,ssp}^{(2)} = L_{yy}(\omega_{SF}) L_{yy}(\omega_{Vis}) L_{zz}(\omega_{IR}) \sin \beta_{IR} \chi_{yyz}^{(2)} \tag{S15}$$

$$\begin{aligned}
\chi_{eff,ppp}^{(2)} = & -L_{xx}(\omega_{SF})L_{xx}(\omega_{Vis})L_{zz}(\omega_{IR})\cos\beta_{SF}\cos\beta_{Vis}\sin\beta_{IR}\chi_{xxz}^{(2)} \\
& -L_{xx}(\omega_{SF})L_{zz}(\omega_{Vis})L_{xx}(\omega_{IR})\cos\beta_{SF}\sin\beta_{Vis}\cos\beta_{IR}\chi_{xzx}^{(2)} \\
& +L_{zz}(\omega_{SF})L_{xx}(\omega_{Vis})L_{xx}(\omega_{IR})\sin\beta_{SF}\cos\beta_{Vis}\cos\beta_{IR}\chi_{zxx}^{(2)} \\
& +L_{zz}(\omega_{SF})L_{zz}(\omega_{Vis})L_{zz}(\omega_{IR})\sin\beta_{SF}\sin\beta_{Vis}\sin\beta_{IR}\chi_{zzz}^{(2)}
\end{aligned} \tag{S16}$$

where  $\beta_{SF}$ ,  $\beta_{Vis}$  and  $\beta_{IR}$  are the angles between the surface normal and the sum frequency beam, the input visible beam, and the input IR beam, respectively.  $L_{ii}$  ( $i = x, y$  or  $z$ ) denotes the Fresnel coefficients. After considering the Fresnel coefficient constants under current experimental geometry, Eqs. (S17)-(S18) are then given by

$$\chi_{eff,ssp}^{(2)} = 1.218\chi_{yyz}^{(2)} \tag{S17}$$

$$\chi_{eff,ppp}^{(2)} = -0.126\chi_{xxz}^{(2)} + 1.088\chi_{zzz}^{(2)} \tag{S18}$$

According to Eqs.(S4)-(S18), the tilt angle ( $\theta$ ) and twist angle can be related to the ppp and ssp spectral intensity ratio of peptide amide I signals by Eqs. (S19)-(S20).

$$\chi_{ssp}^{(2)} = 4.872N_s^t \left[ \left( \frac{1+r}{2} - \frac{(1+\sin 2\psi)\beta_{aca}}{\beta_{ccc}} \right) \langle \cos \theta \rangle - \left( \frac{1-r}{2} - \frac{(1+\sin 2\psi)\beta_{aca}}{\beta_{ccc}} \right) \langle \cos^3 \theta \rangle \right] \beta_{ccc} \tag{S19}$$

$$\begin{aligned}
\chi_{ppp}^{(2)} = & -0.504N_s^t \left[ \left( \frac{1+r}{2} - \frac{(1+\sin 2\psi)\beta_{aca}}{\beta_{ccc}} \right) \langle \cos \theta \rangle - \left( \frac{1-r}{2} - \frac{(1+\sin 2\psi)\beta_{aca}}{\beta_{ccc}} \right) \langle \cos^3 \theta \rangle \right] \beta_{ccc} \\
& + 4.352N_s^t \left[ \left( r + \frac{2(1+\sin 2\psi)\beta_{aca}}{\beta_{ccc}} \right) \langle \cos \theta \rangle + \left( 1-r - \frac{2(1+\sin 2\psi)\beta_{aca}}{\beta_{ccc}} \right) \langle \cos^3 \theta \rangle \right] \beta_{ccc}
\end{aligned} \tag{S20}$$

By applying the bond additivity model,<sup>26-28</sup> the relationship of  $\beta_{aca} = 0.32\beta_{ccc}$ ,  $\beta_{aac} = 0.58\beta_{ccc}$ , is deduced. Fig. 2D and Fig.S2 present a relation between the  $\chi_{ppp}^{(2)}/\chi_{ssp}^{(2)}$  ratio and  $\theta$  for a certain twist angle ( $\psi$ ). Because  $\sin(180^\circ-2\psi)$  equal to  $\sin(2\psi)$ , we only plot the case of  $\psi$  ranging from  $-45^\circ$  to  $45^\circ$  in Fig.2D. It is worth noting that the ratio of  $\chi_{ppp}^{(2)}/\chi_{ssp}^{(2)}$  at any tilt angle is larger than 1.44 for the rotation angle ( $\psi$ ) of  $-10^\circ < \psi < 100^\circ$ , while smaller than 1.44 for  $-80^\circ < \psi < -10^\circ$ . It means that the measured  $\chi(2)$  ppp/ $\chi(2)$  ssp value at  $\text{pH} > 4.3$  always falls below the possible  $\chi(2)$  ppp/ $\chi(2)$  ssp range of  $-80^\circ < \psi < -10^\circ$ . In contrast, the  $\chi(2)$  ppp/ $\chi(2)$  ssp value at  $\text{pH} < 4.3$  falls above the possible range of  $-10^\circ < \psi < 100^\circ$ . The resulting tilt angle fall in the range of  $20^\circ$  to  $33^\circ$  for  $-30^\circ < \psi < -60^\circ$  at  $\text{pH} > 4.3$  (magenta color in Fig. S2), and about  $17^\circ \sim 35^\circ$  for  $90^\circ > \psi > 0^\circ$  at  $\text{pH}=3.3$ , indicating that M2TM has similar rotation angle for the case at  $\text{pH} > 4.3$  and likely rotates its helical axis when the pH changes from  $\text{pH} > 4.3$  to  $\text{pH} < 4.3$ . It is worth mentioning

that the tilt angle will be different for different psi values. For example, for  $\chi^{(2)} \text{ ppp}/\chi^{(2)} \text{ ssp} = 1.2$ , the tilt angle( $\theta$ ) is  $-43^\circ$  for  $\psi = -20^\circ$ , whereas  $\theta = 27^\circ$  for  $\psi = -45^\circ$ , see Table S4.

Table S4. The dependence of the tilt angle ( $\theta$ ) to the rotation angle ( $\psi$ ) for  $\chi^{(2)} \text{ ppp}/\chi^{(2)} \text{ ssp}=1.2$  and 1.65

|  |                                  |     |     |     |     |
|--|----------------------------------|-----|-----|-----|-----|
| $\chi^{(2)} \text{ ppp}/\chi^{(2)} \text{ ssp}=1.2$  | Rotation angle( $\psi$ )(degree) | -20 | -30 | -40 | -45 |
|  | Tilt angle ( $\theta$ )(degree)  | 43  | 31  | 28  | 27  |
| $\chi^{(2)} \text{ ppp}/\chi^{(2)} \text{ ssp}=1.65$ | Rotation angle( $\psi$ )(degree) | 80  | 70  | 60  | 50  |
|  | Tilt angle ( $\theta$ )(degree)  | 24  | 20  | 18  | 17  |

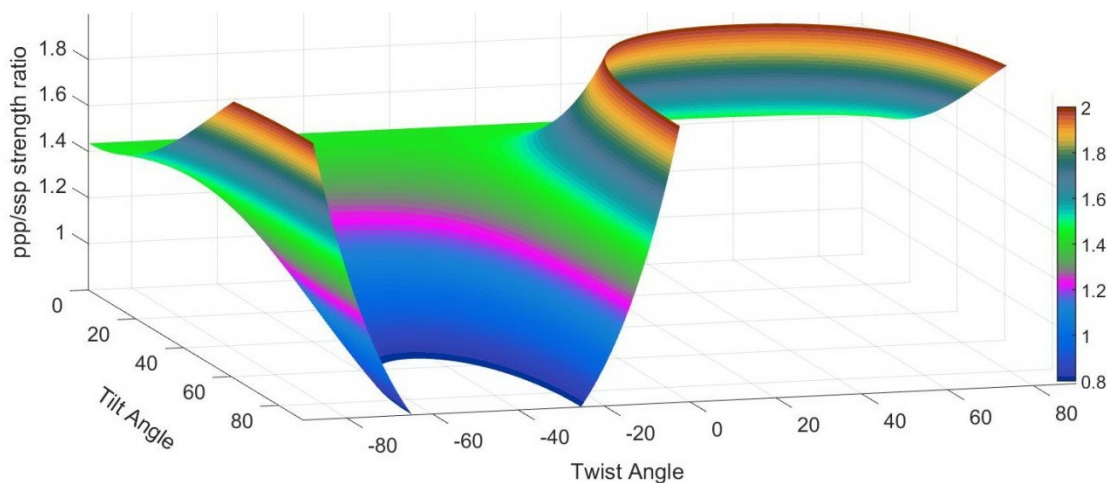


**Fig. S2.** The relationship between  $\chi^{(2)} \text{ ppp}/\chi^{(2)} \text{ ssp}$  of the  $\alpha$ -helix and helix tilt angle ( $\theta$ ) for a certain rotation angle ( $\psi$ ).

When the  $\chi_{\text{ppp}}^{(2)} / \chi_{\text{ssp}}^{(2)}$  ratio is smaller than 1.44, the SFG signal is dominant from the A mode; otherwise, both A mode and  $E_1$  mode contribute to the SFG signal. In addition, it has been reported that the typical frequency of  $E_1$  mode is about  $5 \text{ cm}^{-1}$  higher than that of A mode.<sup>29</sup> Fig. S5C shows that the peak center in the ssp and ppp spectra at pH = 4.6 is lower than that at pH = 3.7, which further confirms that the twist angle differs between these two pH values.

## 5. The SFG spectra of M2

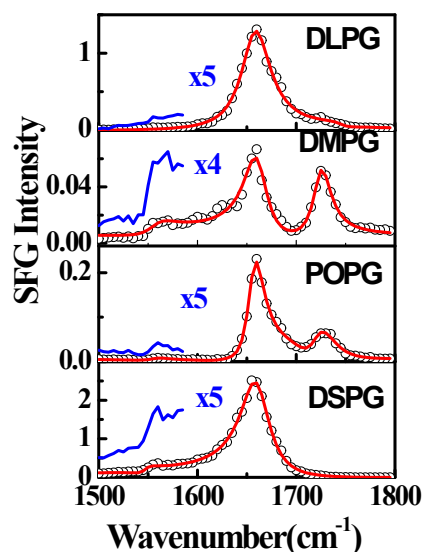


**Fig.S3** The ppp amide I spectra of M2TM in lipid bilayers with different lipid chain lengths at pH  $\sim 6.8$ .

Fig. S3 shows the ppp amide I spectra of M2TM in lipid bilayers with different lipid chain lengths. The spectra are dominated by a strong peak at  $1655 (\pm 5) \text{ cm}^{-1}$  from amide I vibration, which is an indication of an  $\alpha$ -helix or a loop structure.

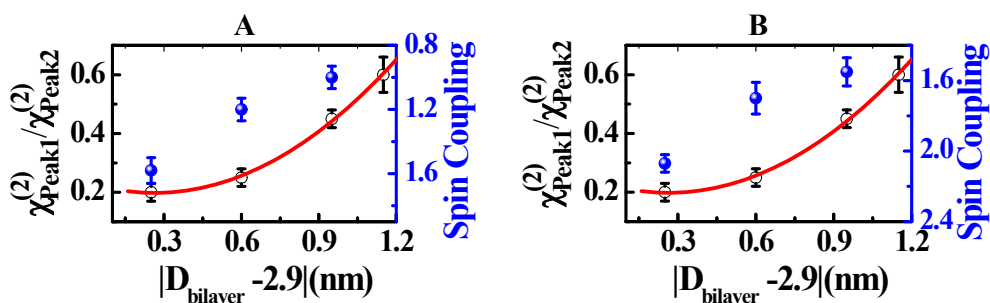


**Fig. S4** Amide III  $\chi(2)$  Peak1/ $\chi(2)$  Peak2 ratio (black empty circle) and spin coupling (blue solid circle) data from previous EPR study<sup>30,31</sup> as a function of the absolute value of bilayer thickness minus 2.9 nm. A) Spin coupling data for PC bilayer; B) Spin coupling data for mixed PC/PG bilayer.

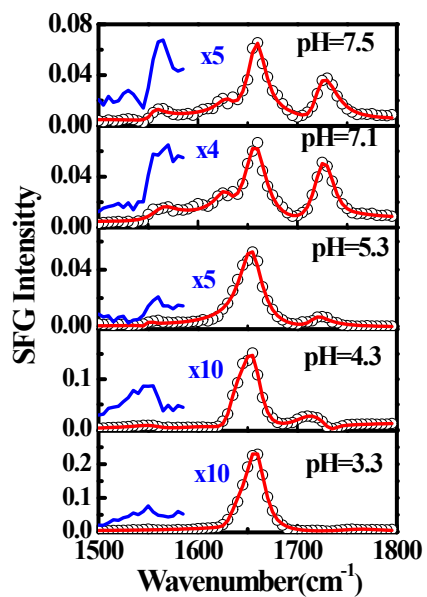


**Fig.S5** The ppp amide I spectra of M2TM in DMPG bilayers prepared at different pH subphases.

Fig. S5 shows the ppp amide I spectra of M2TM in DMPG bilayers prepared at different pH subphases. As the pH value decreases, the  $\sim 1555\text{ cm}^{-1}$  and  $\sim 1720\text{ cm}^{-1}$  peaks become much weaker.

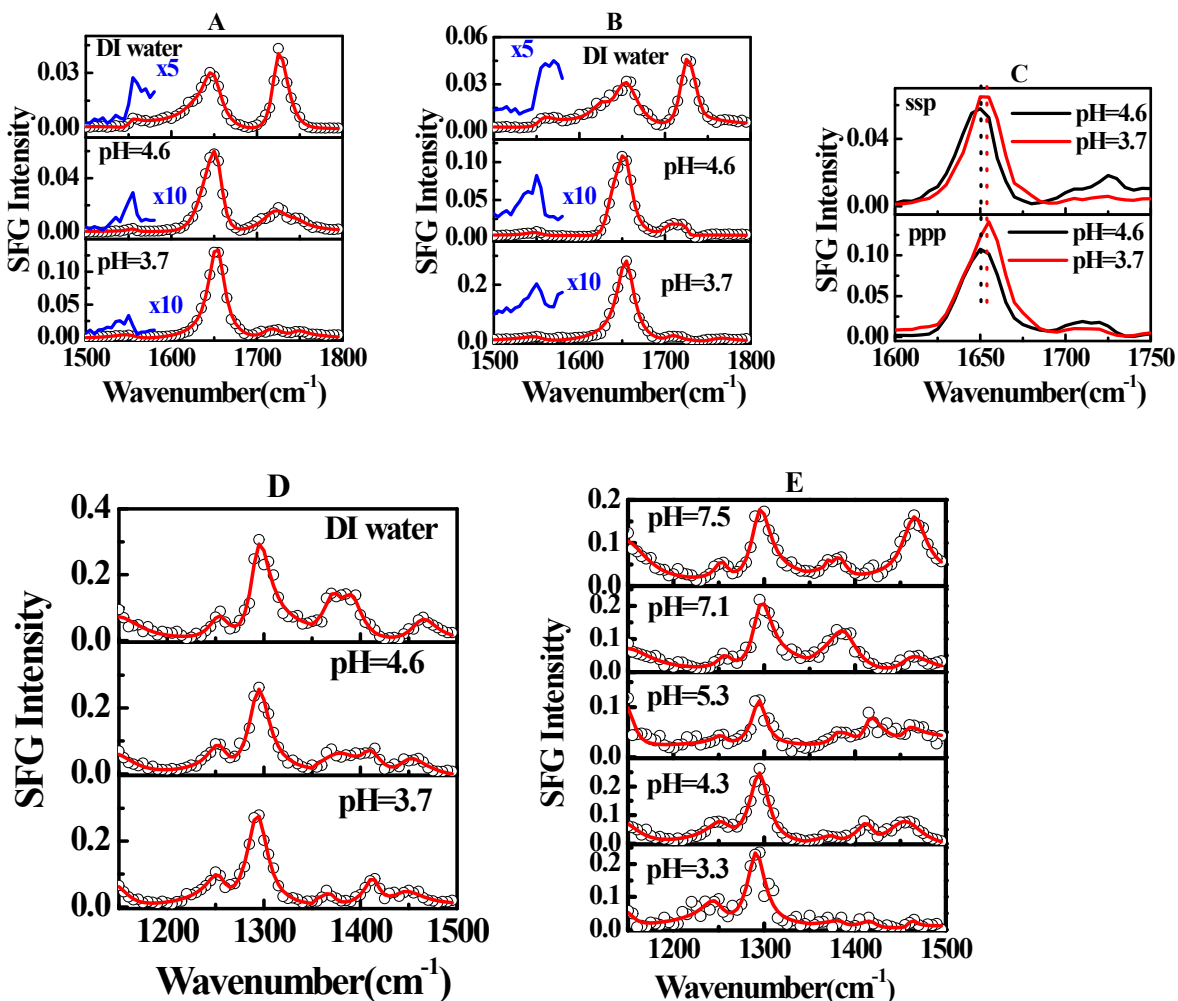


**Fig.S6** Amide I spectra of M2TM in DMPG bilayers at different pH conditions by adding a certain amount of HCl solution: A) ssp and B) ppp. C) A comparison between pH 4.6 and pH 3.7. D) The ssp amide III spectra of M2TM in DMPG bilayers at different pH conditions by adding a certain amount of HCl solution. E). The ssp amide III ssp spectra of M2TM in DMPG bilayer with a subphase pH prepared before the experiment.

In Fig.S6D, in addition to the peaks related to  $\text{CH}_3$  bending mode ( $\sim 1370$  and  $\sim 1465$   $\text{cm}^{-1}$ ), a new peak at  $1415$   $\text{cm}^{-1}$  is observed at pH of 4.6 and 3.7. The  $\sim 1415$   $\text{cm}^{-1}$  band was assigned to the protonated His37( $\text{ImH}^+$ ).<sup>32</sup> The weakening of  $\sim 1555$   $\text{cm}^{-1}$  peak and the appearances of the  $\sim 1415$   $\text{cm}^{-1}$  peaks are the result of the cation- $\pi$  interactions between the protonated His37 imidazole rings and the  $\pi$  electrons of the Trp41 indole ring.<sup>32</sup> These peaks reveal the orientation of Trp41 changes in conjunction with the protonation of His37. Such spectral features are also found in the sample prepared in DMPG bilayer with a subphase pH prepared before the experiment(Fig.S6E).

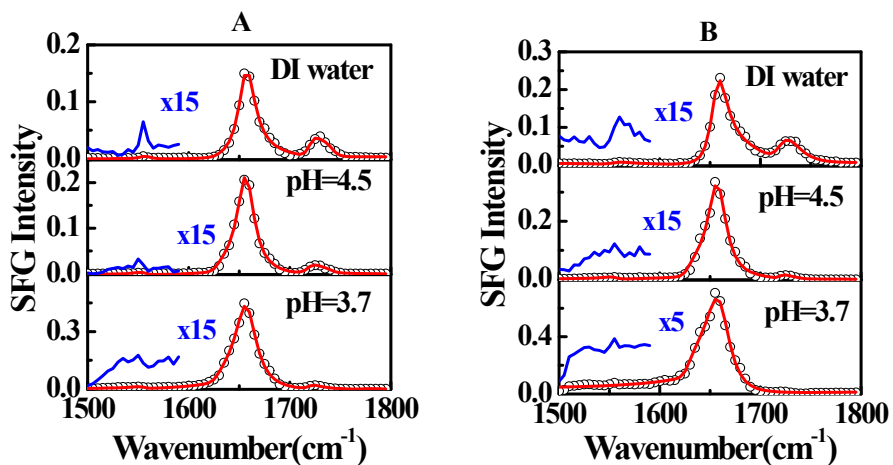


Fig.S7 Amide I spectra of M2TM in POPG bilayers at different pH conditions by adding a certain amount of HCl solution: A) ssp and B) ppp.

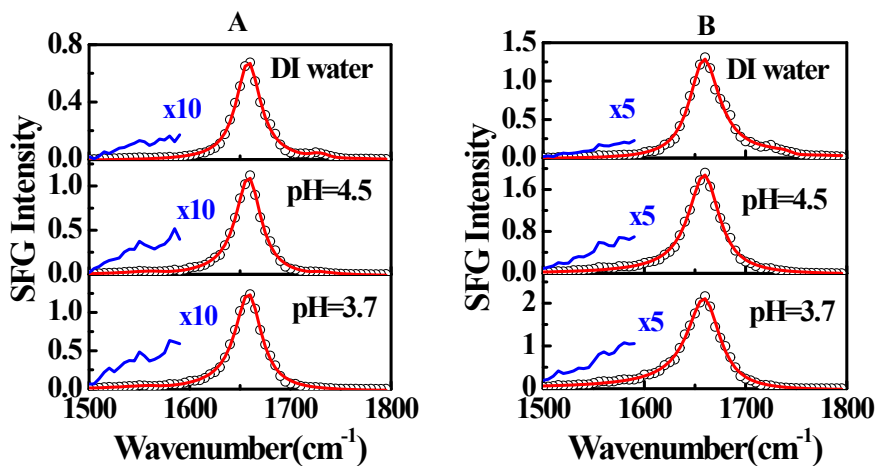
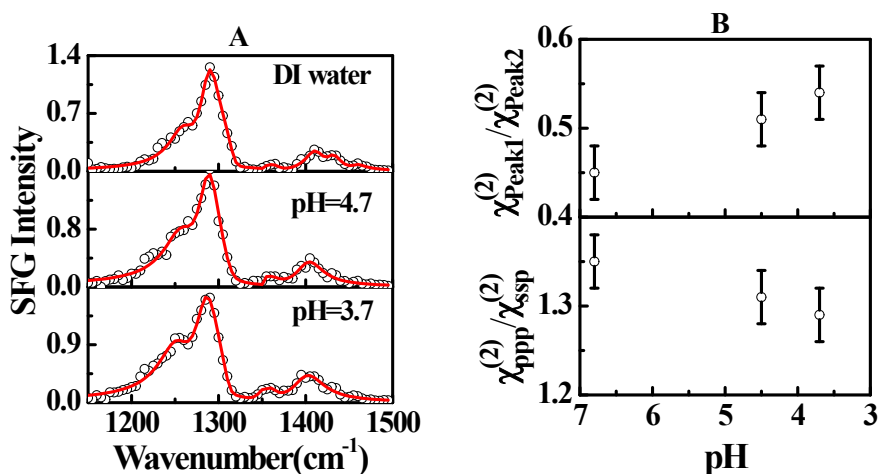


Fig.S8 Amide I spectra of M2TM in DLPG bilayers at different pH conditions by adding a certain amount of HCl solution: A) ssp and B) ppp.



**Fig. S9** A) The ssp amide III spectra of M2TM in DLPG bilayers at different pH conditions by adding a certain amount of HCl solution. B) Fitting strength ratio of  $\chi^{(2)}$  Peak1/ $\chi^{(2)}$  Peak2 and ppp and ssp spectra ( $\chi^{(2)}$  ppp/ $\chi^{(2)}$  ssp) of the  $\sim 1655$  cm<sup>-1</sup> peak as a function of pH value.

#### References

1. H. C. Li, S.J. Ye, F. Wei, S.L. Ma, Y. Luo, *Langmuir*, 2012, **28**, 16979.
2. S.J. Ye, F. Wei, *Analyst*, 2011, **136**, 2489.
3. Y.R. Shen, *The Principles of Nonlinear Optics*. Wiley: New York, 1984.
4. A. Lambert, P. Davies, D. Neivandt, *Appl. Spectrosc. Rev.*, 2005, **40**, 103.
5. J. Wang, S. Kim, F. Kovacs, T.A. Cross, *Protein Sci.*, 2001, **10**, 2241-2250.
6. K. Nishimura, S. Kim, L. Zhang, T.A. Cross, *Biochemistry*, 2002, **41**, 13170-13177.
7. J. Hu, T. Asbury, S. Achuthan, C. Li, R. Bertram, J.R. Quine, R. Fu, T.A. Cross, *Biophys. J.*, 2007, **92**, 4335-4343.
8. S.D. Cady, T.V. Mishanina, M. Hong, *J. Mol. Biol.*, 2009, **385**, 1127-1141.
9. R.M. Pielak, J.R. Schnell, J.J. Chou, *Proc. Natl. Acad. Sci. U. S. A.*, 2009, **106**, 7379-7384.
10. R.M. Pielak, J.R. Schnell, J.J. Chou, *Nature*, 2010, **463**, 689-692.
11. R.M. Pielak, J.J. Chou, *Biochem. Biophys. Res. Commun.*, 2010, **401**, 58-63.
12. M. Sharma, M. Yi, H. Dong, H. Qin, E. Peterson, D.D. Busath, H.X. Zhou, T.A. Cross, *Science*, 2010, **330**, 509-512.
13. J. Wang, Y. Wu, C. Ma, G. Fiorin, J. Wang, L.H. Pinto, R.A. Lamb, M.L. Klein, W.F. Degrado, *Proc. Natl. Acad. Sci. U. S. A.*, 2013, **110**, 1315-1320.

14. Y. Wu, B. Canturk, H. Jo, C. Ma, E. Gianti, M.L. Klein, L.H. Pinto, R.A. Lamb, G. Fiorin, J. Wang, W.F. DeGrado, *J.Am.Chem.Soc.*, 2014, **136**, 17987-17995.
15. L.B. Andreas, M. Reese, M.T. Eddy, V. Gelev, Q.Z. Ni, E.A. Miller, L. Emsley, G. Pintacuda, J.J. Chou, R.G. Griffin, *J.Am.Chem.Soc.*, 2015, **137**, 14877-14886.
16. J.R. Schnell, J.J. Chou, *Nature*, 2008, **451**, 591-595.
17. A.L. Stouffer, R. Acharya, D. Salom, A.S. Levine, L. Di Costanzo, C.S. Soto, V. Tereshko, V. Nanda, S. Stayrook, W.F. DeGrado, *Nature*, 2008, **451**, 596-599.
18. R. Acharya, V. Carnevale, G. Fiorin, B.G. Levine, A.L. Polishchuk, V. Balannik, I. Samish, R.A. Lamb, L.H. Pinto, W.F. DeGrado, M.L. Klein, *Proc. Natl. Acad. Sci. U. S. A.*, 2010, **107**, 15075-15080.
19. J.L. Thomaston, M. Alfonso-Prieto, R.A. Woldeyes, J.S. Fraser, M.L. Klein, G. Fiorin, W.F. DeGrado, *Proc. Natl. Acad. Sci. U. S. A.*, 2015, **112**, 4260-14265.
20. J.L. Thomaston, W.F. DeGrado, *Protein Sci.*, 2016, **25**, 1551-1554.
21. S.D. Cady, C. Goodman, C.D. Tatko, W.F. DeGrado, M. Hong, *J. Am. Chem. Soc.*, 2007, **129**, 5719-5729.
22. F.A. Kovacs, J.K. Denny, Z. Song, J.R. Quine, T.A. Cross, *J. Mol. Biol.*, 2000, **295**, 117-125
23. C.L. Tian, P.F. Gao, L.H. Pinto, R.A. Lamb, T.A. Cross, *Protein Sci.*, 2003, **12**, 2597-2605.
24. A. Kukol, P.D. Adams, L.M. Rice, A.T. Brunger, I.T. Arkin, *J. Mol. Biol.*, 1999, **286**, 951-962.
25. A. J. Moad, G. J. Simpson, *J. Phys. Chem. B*, 2004, **108**, 3548-3562.
26. K. T. Nguyen, S. Le Clair, S.J. Ye, Z. Chen, *J. Phys. Chem. B*, 2009, **113**, 12169-12180.
27. J. Wang, S. H. Lee, Z. Chen, *J. Phys. Chem. B*, 2008, **112**, 2281-2290.
28. X.Y. Chen, J. Wang, A.P. Boughton, C.B. Kristalyn, Z. Chen, *J.Am. Chem.Soc.*, 2007, **129**, 1420-1427.
29. D. Marsh, M. Muller, F.-J. Schmitt, *Biophys. J.*, 2000, **78**, 2499-2510.
30. K.C. Duong-Ly, V. Nanda, W.F. Degrad, K.P. Howard, *Protein Sci.*, 2005, **14**, 856.
31. K. Saotome, K.C. Duong-Ly, K.P. Howard, *Biopolymers*, 2015, **104**, 405.
32. A. Okada, T. Miura, H. Takeuchi, *Biochemistry*, 2001, **40**, 6053.